

# Decentralized Optimal Control of Connected and Automated Vehicles in a Corridor

Liuhui Zhao *Member, IEEE*, Andreas A. Malikopoulos, *Senior Member, IEEE*

**Abstract**—In earlier work, we established a decentralized optimal control framework for coordinating online connected and automated vehicles (CAVs) in specific transportation segments, e.g., urban intersections, merging roadways, roundabouts, and speed reduction zones. In this paper, we address coordination of CAVs in a corridor with multiple such scenarios and derive a closed-form analytical solution that includes interior boundary conditions. We evaluate the effectiveness of the solution through simulation in VISSIM. The proposed approach reduces significantly both fuel consumption and travel time for the CAVs compared to the baseline scenario where traditional human-driven vehicles without control are considered.

## I. INTRODUCTION

Urban intersections, merging roadways, roundabouts, and speed reduction zones along with the driver responses to various disturbances [1] are the primary sources of bottlenecks that contribute to traffic congestion. Connectivity and automation in vehicles provide the most intriguing opportunity for enabling users to better monitor transportation network conditions and make better operating decisions. Several research efforts have been reported in the literature proposing different approaches on coordinating CAVs at different transportation segments, e.g., urban intersections, merging roadways, roundabouts, and speed reduction zones, with the intention to improve transportation efficiency. In 2004, Dresner and Stone [2] proposed the use of the reservation scheme to control a single intersection of two roads with vehicles traveling with similar speed on a single direction on each road, i.e., no turns are allowed. Since then, numerous approaches have been reported in the literature [3]–[5], to achieve safe and efficient control of traffic through intersections including extensions of the reservation scheme in [2]. Some approaches have focused on coordinating vehicles at intersections to improve the traffic flow [6]–[8]. A detailed discussion of the research efforts in this area that have been reported in the literature to date can be found in [9].

Although previous research aimed at enhancing our understanding of improving emerging transportation systems just a few efforts have reported results on corridors [10] that include multiple intersections and merging roadways. More recently, a control framework was developed for a coordinated and integrated corridor management in a mixed traffic environment, where CAVs send information to a centralized

traffic operation center and received control actions from the center to improve network-wide traffic flow [11], [12].

In earlier work, a decentralized optimal control framework was established for coordinating online CAVs in different transportation segments. A closed-form, analytical solution without considering state and control constraints was presented in [13], [14], and [15] for coordinating online CAVs at highway on-ramps, in [16] at two adjacent intersections, and in [17] at roundabouts. The solution of the unconstrained problem was also validated experimentally at the University of Delaware’s Scaled Smart City using ten robotic CAVs [18] in a merging roadway scenario. The solution of the optimal control problem considering state and control constraints was presented in [19] at an urban intersection without considering rear-end collision avoidance constraint, and the conditions under which the latter does not become active were presented in [20].

In this paper, we consider coordination of a number of CAVs through a corridor. To ensure that no lateral collision occurs, we impose interior constraints in our Hamiltonian analysis and derive the optimal solution throughout the entire corridor.

The paper is organized as follows. In Section II, we formulate the problem and provide the modeling framework. In Section III, we derive the analytical, closed form solution with interior constraints. In Section IV, we validate the effectiveness of the analytical solution in a simulation environment and conduct a comparison analysis with traditional human-driven vehicles. Finally, the concluding remarks and discussion are provided in Section V.

## II. PROBLEM FORMULATION

We consider a corridor (Fig. 1) that consists of three merging zones, e.g., two merging roadways and one urban intersection. The corridor has a coordinator that can monitor the vehicles traveling along the corridor within a *control zone* (shown with a dashed box in Fig. 1). Note that the coordinator serves as an information center which is able to collect vehicular data through vehicle-to-infrastructure and is not involved in any decision on the vehicle operation. Road side units could be placed in each merging zone and used to transmit data between vehicles and the coordinator. Thus, the coverage of the coordinator is flexible and the length of corridor could be extended in the presence of connected infrastructure.

Let  $N(t) \in \mathbb{N}$  be the number of CAVs in the corridor at time  $t \in \mathbb{R}^+$  and  $M \in \mathbb{M}$  be the number of merging zones along the corridor where lateral collisions may occur. When

This research was supported by ARPAA’s NEXTCAR program under the award number DE-AR0000796.

The authors are with the Department of Mechanical Engineering, University of Delaware, Newark, DE 19716 USA (emails: lhzha@udel.edu; andreas@udel.edu.)

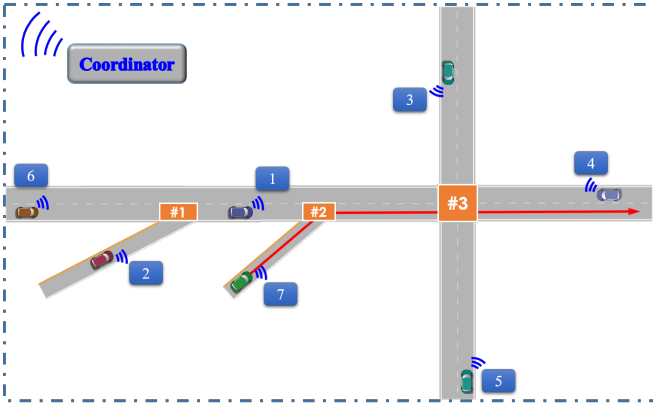


Fig. 1. Corridor with connected and automated vehicles.

as a vehicle enters the control zone of the corridor, it broadcasts its origin-destination (OD) to the coordinator. Then, the coordinator assigns a unique number  $i = 1, \dots, N(t) \in \mathbb{N}$  (Fig. 1) that serves as an identification of the vehicles within the control zone. The policy through which the sequence that each vehicle crosses each merging zone throughout the corridor may be the result of a higher level optimization problem, which is not addressed in this paper. In what follows, we will adopt a specific scheme for determining this sequence of the vehicles crosses each merging zone throughout the corridor but we emphasize that our analysis is not restricted to this sequence.

To avoid any possible lateral collision while the vehicles crossing the merging zones, once a vehicle  $i$  enters the control zone, it computes the time that will be entering each merging zone which is discussed in the next Section. Let  $t_i^0$  be the initial time that vehicle  $i$  enters the control zone of the corridor,  $t_i^{m_j}$  be the time that vehicle  $i$  enters the merging zone  $j$ ,  $j \in M$ , and  $t_i^f$  be the time that vehicle  $i$  exits the last merging zone along its route. In what follows, we provide a policy for the vehicle sequence crossing the merging zones in the corridor. The focus is on the lower level control problem that yields for each vehicle the optimal control input (acceleration/deceleration) to achieve the assigned  $t_i^{m_j}$  using a given policy that designates  $t_i^{m_j}$  (upon arrival of CAV  $i$  at the entry of the control zone).

#### A. Vehicle Model and Constraints

For simplicity, each vehicle is modeled as a double integrator

$$\begin{aligned} \dot{p}_i &= v_i(t) \\ \dot{v}_i &= u_i(t) \end{aligned} \quad (1)$$

where  $p_i(t) \in \mathcal{P}_i$ ,  $v_i(t) \in \mathcal{V}_i$ , and  $u_i(t) \in \mathcal{U}_i$  denote the position, speed and acceleration/deceleration (control input) of each vehicle  $i$  in the corridor. The sets  $\mathcal{P}_i$ ,  $\mathcal{V}_i$ , and  $\mathcal{U}_i$ ,  $i = 1, \dots, N(t) \in \mathbb{N}$ , are complete and totally bounded subsets of  $\mathbb{R}$ . Let  $x_i(t) = [p_i(t) \ v_i(t)]^T$  denote the state of each vehicle  $i$ , with initial value  $x_i^0 = [p_i^0 \ v_i^0]^T$ , where  $p_i^0 = p_i(t_i^0) = 0$  is the position of the vehicle at the entry of the corridor, taking values in  $\mathcal{X}_i = \mathcal{P}_i \times \mathcal{V}_i$ .

To ensure that the control input and vehicle speed are within a given admissible range, the following constraints are imposed.

$$\begin{aligned} u_{i,min} &\leq u_i(t) \leq u_{i,max}, \quad \text{and} \\ 0 &\leq v_{min} \leq v_i(t) \leq v_{max}, \quad \forall t \in [t_i^0, t_i^f], \end{aligned} \quad (2)$$

where  $u_{i,min}$ ,  $u_{i,max}$  are the minimum deceleration and maximum acceleration for each vehicle  $i = 1, \dots, N(t) \in \mathbb{N}$ , and  $v_{min}$ ,  $v_{max}$  are the minimum and maximum speed limits respectively.

To ensure the absence of rear-end collision of two consecutive vehicles traveling on the same lane, the position of the preceding vehicle should be greater than or equal to the position of the following vehicle plus a predefined safe distance  $\delta_i(t)$ . Thus we impose the rear-end safety constraint

$$s_i(t) = \xi_i \cdot (p_k(t) - p_i(t)) \geq \delta_i(t), \quad \forall t \in [t_i^0, t_i^f], \quad (3)$$

where  $s_i(t) \in \mathcal{S}_i$  denotes the distance of vehicle  $i$  from the vehicle  $k$  which is physically located ahead of  $i$ . Relate the minimum safe distance  $\delta_i(t)$  as a function of speed  $v_i(t)$ ,

$$\delta_i(t) = \gamma_i + \rho_i \cdot v_i(t), \quad \forall t \in [t_i^0, t_i^f], \quad (4)$$

where  $\gamma_i$  is the standstill distance, and  $\rho_i$  is minimum time gap that vehicle  $i$  would maintain while following another vehicle.

#### B. Policy for Vehicle Sequence Crossing the Merging Zones

In the modeling framework described above, we assume that the vehicles traveling in the corridor do not change lanes except to make necessary turns. When a vehicle  $i$  enters the control zone of the corridor it computes the time  $t_i^{m_j}$  for each merging zone  $j$  based on the following three subsets: 1)  $\mathcal{S}_i$  contains all vehicles share the same route with vehicle  $i$ , 2)  $\mathcal{L}_i$  contains all vehicles that travel in the same lane in merging zone  $j$  with vehicle  $i$  but travel from different routes (i.e., may have rear-end collision with vehicle  $i$  in merging zone  $j$ , but lateral collision in the immediate upstream merging zone  $j-1$ ), and 3)  $\mathcal{C}_i$  contains all vehicles from different entry links in merging zone  $j$  that may have lateral collision with vehicle  $i$ .

To ensure that (3) is satisfied at  $t_i^{m_j}$ , we first impose the following condition

$$t_i^{m_j} = \max \left\{ \min \left\{ t_k^{m_j} + \rho_i, \frac{p_j(t)}{v_{min}} + t_i^0 \right\}, \frac{p_j(t)}{v_i^0} + t_i^0, \frac{p_j(t)}{v_{max}} + t_i^0 \right\}, \quad (5)$$

where  $t_k^{m_j}$  is the time when the vehicle  $k$  enters merging zone  $j$ ,  $k \in \mathcal{S}_i$ ,  $p_j(t)$  is the distance from the entry point of the control zone until the entry of merging zone  $j$ , and  $v_i^0$  is the initial speed of vehicle  $i$  when it enters the control zone of the corridor. If  $\mathcal{L}_i$  is not empty, we impose an additional constraint for the time  $t_i^{m_j}$ :

$$(t_i^{m_j} - t_e^{m_j}) \cdot (t_i^{m_{j-1}} - t_e^{m_{j-1}}) > 0 \quad (6)$$

where  $t_e^{m_j}$  is the time when the vehicle  $e$  enters zone  $j$ ,  $e \in \mathcal{L}_i$ .

To avoid lateral collision in the merging zone  $j$ , we need to adjust  $t_i^{m_j}$  from (5) with or without the constraint imposed by (6) based on the time that each vehicle computes  $t_i^{m_j}$  in set  $\mathcal{C}_i$  as follows.

---

```

1 initialize set  $A \leftarrow \emptyset$ , variable  $t_i^{m_j^*} \leftarrow 0$ ;
2 find  $A \leftarrow \{t_o^{m_j} : t_o^{m_j} \geq t_i^{m_j}, \forall o \in \mathcal{C}_i\}$ ;
3 if  $A = \emptyset$ , then
     $A \leftarrow \{t_o^{m_j}, \forall o \in \mathcal{C}_i\}$ ,
     $t_i^{m_j^*} \leftarrow \max\{\max\{A\} + \rho_i, t_i^{m_j}\}$ ;
else
    if  $t_i^{m_j} + \rho_i \leq \min\{A\}$ , then  $t_i^{m_j^*} \leftarrow t_i^{m_j}$ ;
    else
        for  $z \leftarrow 1$  to  $N(A) - 1$  :
            if  $t_z^{m_j} + \rho_i \leq t_{z+1}^{m_j} - \rho_i$ ,
                then  $t_i^{m_j^*} \leftarrow t_z^{m_j} + \rho_i$ ;
            end
        end
        if  $t_i^{m_j^*} = 0$ , then  $t_i^{m_j^*} \leftarrow \max\{A\} + \rho_i$ 
        end
    end
end
end
end
4  $t_i^{m_j} \leftarrow t_i^{m_j^*}$ .

```

---

Each vehicle follows the above policy to compute the time  $t_i^{m_j}$  that will be entering the merging zone  $j \in M$  upon arrival of vehicle  $i$  in the entry of the control zone of the corridor. In what follows, we will provide the closed-form solution of the optimal control problem for each vehicle  $i = 1, \dots, N(t) \in \mathbb{N}$ .

### III. ANALYTICAL SOLUTION

#### A. Analytical Solution for the Unconstrained Problem

For each vehicle  $i = 1, \dots, N(t) \in \mathbb{N}$ , we define the cost functional  $J_i(u(t))$  which is the  $L^2$ -norm of the control input in  $[t_i^0, t_i^f]$

$$J_i(u(t)) = \frac{1}{2} \int_{t_i^0}^{t_i^f} u_i^2(t) dt, \quad (7)$$

subject to : (1), (2), (3),  $p_i(t_i^0) = 0$ ,  $p_i(t_i^{m_j}) = p_j$ ,  
and given  $t_i^0, v_i^0, t_i^{m_j}$ .

To simplify the analysis we do not consider the state and control constraints (2). The constrained problem formulation has been addressed in [19], and it requires the constrained and unconstrained arcs of the state and control input to be pieced together to satisfy the Euler-Lagrange equations and necessary condition of optimality. So our approach yields the optimal solution as long as the control input and speed of each vehicle is within the imposed limits.

From (7) and the state equations (1), for each vehicle  $i = 1, \dots, N(t) \in \mathbb{N}$  the Hamiltonian function with the state and control adjoined is

$$H_i(t, p_i(t), v_i(t), u_i(t)) = \frac{1}{2} u(t)_i^2 + \lambda_i^p \cdot v_i(t) + \lambda_i^v \cdot u_i(t), \quad (8)$$

where  $\lambda_i^p$  and  $\lambda_i^v$  are the costate components.

When the inequality state and control constraints are not active, applying the necessary condition, the optimal control can be given

$$u_i(t) + \lambda_i^v = 0, \quad i \in \mathcal{N}(t). \quad (9)$$

From the Euler-Lagrange equations we have  $\lambda_i^p(t) = a_i$ , and  $\lambda_i^v(t) = -(a_i \cdot t + b_i)$ . The coefficients  $a_i$  and  $b_i$  are constants of integration corresponding to each vehicle  $i$ . From (9) the optimal control input (acceleration/deceleration) as a function of time is given by

$$u_i^*(t) = a_i \cdot t + b_i, \quad \forall t \geq t_i^0. \quad (10)$$

Substituting the last equation into (1) we find the optimal speed and position for each vehicle, namely  $v_i^*(t) = \frac{1}{2} a_i \cdot t^2 + b_i \cdot t + c_i$ ,  $p_i^*(t) = \frac{1}{6} a_i \cdot t^3 + \frac{1}{2} b_i \cdot t^2 + c_i \cdot t + d_i$ ,  $\forall t \geq t_i^0$ . where  $d_i$  and  $e_i$  are constants of integration. The constants of integration  $a_i$ ,  $c_i$ ,  $d_i$ , and  $e_i$  are computed at each time  $t$ ,  $t_i^0 \leq t \leq t_i^f$ , using the values of the control input, speed, and position of each vehicle  $i$  at  $t$ , the position  $p_i(t_i^f)$ , and the values of the one of terminal transversality condition, i.e.,  $\lambda_i^v(t_i^f)$ . Since the terminal cost, i.e., the control input, at  $t_i^f$  is zero, we can assign  $\lambda_i^v(t_i^f) = 0$ . To derive online the optimal control for each vehicle  $i$ , we need to update the integration constants at each time  $t$ . We form the following system of four equations, namely

$$\begin{pmatrix} \frac{t^2}{2} & t & 1 & 0 \\ \frac{t^3}{6} & \frac{t^2}{2} & t & 1 \\ \frac{(t_i^f)^3}{6} & \frac{(t_i^f)^2}{2} & t_i^f & 1 \\ -t_i^f & -1 & 0 & 0 \end{pmatrix} \cdot \begin{pmatrix} a_i \\ b_i \\ c_i \\ d_i \end{pmatrix} = \begin{pmatrix} v_i(t) \\ p_i(t) \\ p_i(t_i^f) \\ \lambda_i^v(t_i^f) \end{pmatrix}, \quad \forall t \geq t_i^0. \quad (11)$$

#### B. Analytical Solution with Interior Constraints

We consider the general case where the path of vehicle  $i$  consists of more than one merging zone, e.g., vehicle  $i$  enters from the first ramp and travels through #2 and #3 (Fig. 1). Between the time  $t_i^0$  that the vehicle enters the control zone and the time  $t_i^f$  that the vehicle exits the merging zone #3, vehicle  $i$  has to travel across the merging zones #1 and #2 at the designated time  $t_i^{m_1}$  and  $t_i^{m_2}$  respectively. So, we need to impose interior boundary conditions. For the merging zone #1, we have  $p_i(t_i^{m_1}) = p_1$ . If a speed limit is imposed as an interior boundary condition, then we have also  $v_i(t_i^{m_1}) = v_1$ . Let  $t_i^{m_1^-}$  and  $t_i^{m_1^+}$  represents the time just before and after the interior condition. Then

$$\lambda_i^p(t_i^{m_1^-}) = \lambda_i^p(t_i^{m_1^+}) + \pi_0, \quad (12)$$

$$\lambda_i^v(t_i^{m_1^-}) = \lambda_i^v(t_i^{m_1^+}) + \pi_1, \quad (13)$$

$$H^- = H^+ - \pi_0 \cdot v_i(t_i^{m_1}) - \pi_1 \cdot u_i(t_i^{m_1}). \quad (14)$$

where  $\pi_0$  and  $\pi_1$  are constant Lagrange multipliers, determined so that the interior boundary conditions are satisfied. Eq. (12), (13), and (14) imply discontinuities in the position and speed costates and the Hamiltonian at  $t_i^{m_1}$ . The two arcs, i.e., equations before and after  $t_i^{m_1}$ , are pieced together to

solve the problem including the constants of integration,  $\pi_0$  and/or  $\pi_1$ , and the corresponding equations: the initial conditions, the interior boundary conditions the final conditions, i.e.,  $\lambda_i(t_i^f)$ ,  $p_i(t_i^f)$ , and the junction points defined in (12) and (13). To derive online the optimal control for each vehicle  $i$ , we need to update the integration constants at each time  $t$ , so that the controller yields the optimal control online for each vehicle  $i$ , with feedback provided through the re-calculation of the constants of integration for each arc. We form the following system of nine equations, namely

$$\begin{pmatrix} \frac{t^2}{2} & t & 1 & 0 & 0 & 0 & 0 & 0 & 0 \\ \frac{t^3}{6} & \frac{t^2}{2} & t & 1 & 0 & 0 & 0 & 0 & 0 \\ \frac{(t_i^{m_1})^3}{6} & \frac{(t_i^{m_1})^2}{2} & t_i^{m_1} & 1 & 0 & 0 & 0 & 0 & 0 \\ \frac{(t_i^{m_1})^2}{2} & t_i^{m_1} & 1 & 0 & -\frac{(t_i^{m_1})^2}{2} & -t_i^{m_1} & -1 & 0 & 0 \\ 0 & 0 & 0 & 0 & \frac{(t_i^f)^3}{6} & \frac{(t_i^f)^2}{2} & t_i^f & 1 & 0 \\ 0 & 0 & 0 & 0 & -t_i^f & -1 & 0 & 0 & 0 \\ 0 & 0 & 0 & 0 & \frac{(t_i^{m_1})^3}{6} & \frac{(t_i^{m_1})^2}{2} & t_i^{m_1} & 1 & 0 \\ t_i^{m_1} & 1 & 0 & 0 & -t_i^{m_1} & -1 & 0 & 0 & 0 \\ 1 & 0 & 0 & 0 & -1 & 0 & 0 & 0 & -1 \end{pmatrix} \cdot \begin{pmatrix} a_i \\ b_i \\ c_i \\ d_i \\ g_i \\ h_i \\ q_i \\ w_i \\ \pi_0 \end{pmatrix} = \begin{pmatrix} v_i(t) \\ p_i(t) \\ p_i(t_i^{m_1}) \\ 0 \\ p_i(t_i^f) \\ \lambda_i^v(t_i^f) \\ p_i(t_i^{m_1}) \\ 0 \\ 0 \end{pmatrix}, \forall t \geq t_i^0. \quad (15)$$

where  $a_i, b_i, c_i, d_i$  are the constants of integration for the first arc, and  $g_i, h_i, q_i, w_i$  are the constants of integration for the second arc. The analysis for the merging zone #2 can be derived in a similar fashion.

#### IV. SIMULATION RESULTS

To validate the effectiveness of the analytical solution, we create a simple case study in MATLAB that includes two adjacent intersections. The vehicle starts at the beginning of a path with length of 430 m, where the initial speed 12.5 m/s. The first intersection is located at 100 m, and the second one is at 230 m. We are given the times  $t_1, t_2$  that the vehicle will be entering the first and second merging zones as well as the time  $t_f$  that the vehicle will exiting the second merging zone as designated by a higher level optimization problem. In this scenario we consider  $t_1 = 7s, t_2 = 21s$ , and  $t_f = 38s$ . Vehicle position, speed and acceleration profiles without any interior speed constraints are shown in Fig. 2 b). Three acceleration arcs are pieced together for the entire corridor due to the existence of two intermediate intersections, resulting in smooth speed transitions. Assuming that there is one designated speed at each intersection (i.e.,  $v_1 = 12.5m/s$ , and  $v_2 = 15m/s$ ), the

speed costate is discontinuous as indicated with non-zero  $\pi_1$  in (12). Fig. 2a) shows that the acceleration jumps at the intersections.

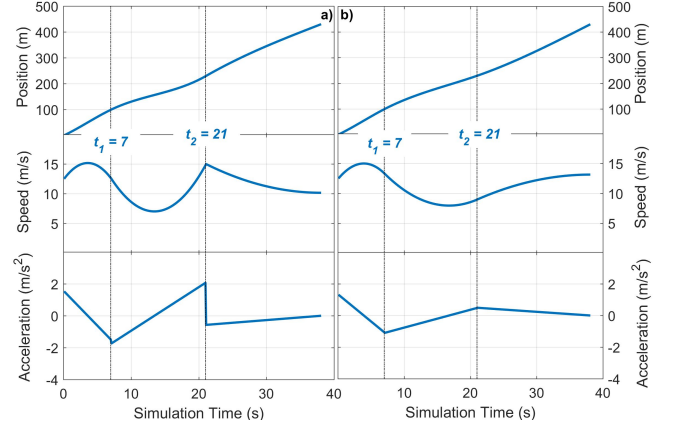


Fig. 2. Optimal trajectory traveling through two intersections.

#### A. Traffic Simulation

In this case study, we create a network of MCity in VISSIM environment, where the corridor consists of one merging at highway on ramp, one roundabout, and one intersection (Fig. 3). Vehicles enter the network on the ramp, join the traffic on the highway with desired speed of 20 m/s, then travel through the roundabout and intersection, where a reduced speed limit of 15.6 m/s, until the end of the path. To evaluate the network performance with the proposed control algorithm, we develop two scenarios (i.e., 0% and 100% CAV market penetration). For the 0% CAV penetration scenario (i.e., baseline scenario), the Wiedemann car following model [21] built in VISSIM is applied. The intersection is controlled by fixed-time signal controller, whose signal timing is optimized for given traffic conditions. The simulation duration is 900 s, and the network serves around 400 vehicles. To accommodate stochastic components of traffic and drive behaviors, we conduct 5 simulation runs for each scenario. Through VISSIM interface, we collected evaluation data at each merging zone, including average traffic speed, delay, CO emission, and fuel consumption every 30 s.

1) *Average Speed*: As we can see from Fig. 4a, because of smooth vehicle movement under the optimal control operation in the merging zone #1, the fluctuation in average speed is reduced for both primary road and ramp. The improvement in traffic speed is marginal considering low traffic flow on both roadways. However, in zone #2, which receives the traffic flow towards the roundabout and also all the traffic from zone #1, traffic condition in the baseline scenario (Fig. 4b) is even worse with large fluctuations. In some cases, uncontrolled merging vehicles may achieve higher speed than those under optimal control, if there is low circulating flow inside the roundabout. Thus, we can see that for several time interval, the average speed under baseline scenario is higher than that under optimal control



Fig. 3. The corridor in MCity.

scenario in (Fig. 4b). With upstream traffic flow, the number of eastbound vehicles arriving at the intersection (i.e., zone #3) is much higher than other traveling directions, which creates congestion that may even propagate to the upstream roundabout. Also, under baseline scenario with fixed-time signal controller, the average speed ranges between 5 m/s and 15 m/s because of stopping for the red lights (Fig. 4c). Through eliminating the stop-and-go driving and removing the signal controller, the CAVs are able to achieve higher travel speed.

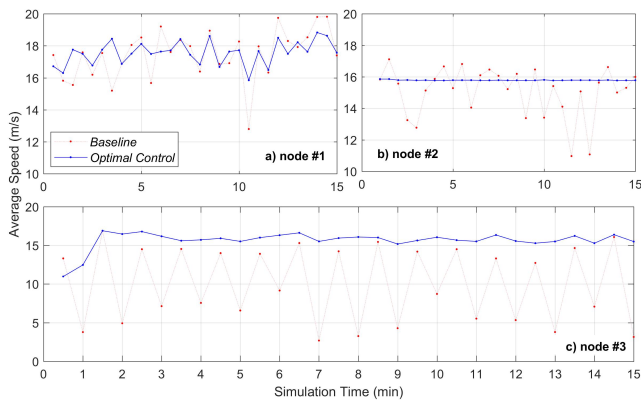


Fig. 4. Average speed in each merging zone.

2) *Total Delay*: The average delay in each zone is collected in VISSIM, and the total delay is calculating by multiplying it by the total number of vehicles processed during each collecting interval. From Fig. 5, we can see a

clear increasing delay farther downstream of the corridor, due to higher traffic volume and signal controller in zone #3. However, with the optimal control, the vehicles are coordinated from the beginning of the corridor, such that the traffic flow feeding into zone #3 is relatively stable. As a result, although there are still minor delays upstream in zones #1 and #2, the delay in zone #3 is negligible, which is in contrast to the baseline scenario where traffic condition gets worse downstream in zone #3.

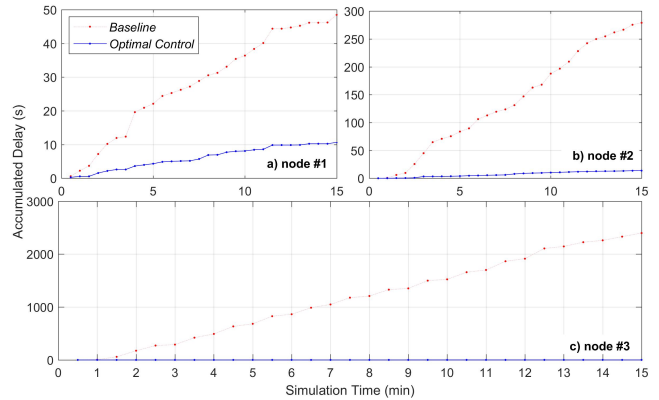


Fig. 5. Accumulated delay in each zone.

3) *Accumulative Fuel Consumption*: Relating fuel consumption to the delay and stops, the trends of total fuel consumption over time are similar to the total delay for each zone. Since traffic control are at the place to regulate traffic under the baseline scenario, i.e., yielding in zone #2 for the roundabout merging, and signal controller in zone #3 for intersection control, and the traffic volume increases, the fuel consumption is much higher at these downstream zones than in zone #1. Similarly, whereas less control efforts in zone #1 leads to marginal fuel savings (Fig. 6a), we achieve high fuel savings in zones #2 and #3 (Fig. 6b and 6c) through fully controlling of CAV movements. The summarized improvements of a network of CAVs over that of non-CAVs are included in Table IV-A.3.

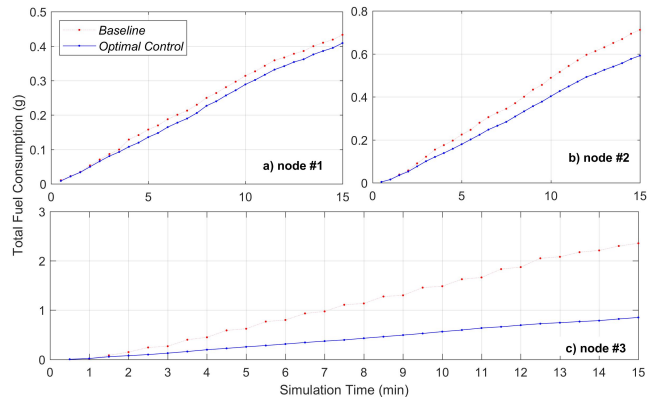


Fig. 6. Accumulated fuel consumption for each zone.

4) *The corridor travel time*: We calculate the average travel times for the vehicles traveling from the ramp through

TABLE I

DIFFERENCES IN MEASURE OF EFFECTIVENESS BETWEEN CAVS AND NON-CAVS.

Zone	Fuel Consumption (%)	CO Emission (%)	Total Delay (%)	Average Speed (%)
1	-6	-5	-78	+0
2	-17	-16	-95	+4
3	-64	-65	-99	+55

merging zones #1 to #3 on the route. Shown in Fig. 7, the large fluctuation in the average travel time under baseline scenario is due to red/green light process. Because of the stop-and-go driving situation under the baseline scenario, the average travel time for the corridor is higher than the one corresponding to optimal control. On average, there is around 8% savings on average travel time and 11% savings on total for the ramp vehicles only through optimal coordination of CAVs.

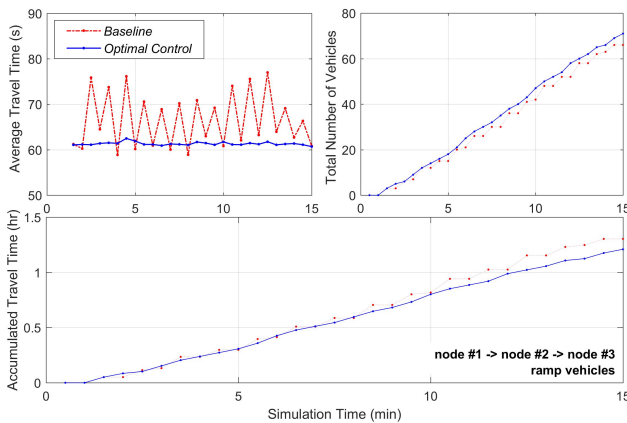


Fig. 7. Travel time performance of the corridor.

## V. CONCLUDING REMARKS AND DISCUSSION

In this paper, we investigated the optimal coordination of CAVs in a corridor. We derived a closed-form analytical solution that considers interior boundary conditions, which provide optimal trajectory for the entire route assigned to the vehicle. The simulation analysis showed the optimal solution can effectively improve network performance. Through vehicle coordination, stop-and-go driving is eliminated, the corridor traffic condition is substantially improved, achieving less fuel consumption and average travel time per vehicle. The state and control constraints were not incorporated in this paper. Ongoing efforts consider the complete solution that includes state and control constraints. Future research should focus on vehicle coordination under mixed traffic environment that include interactions between human-driving vehicles and CAVs.

## REFERENCES

- [1] A. A. Malikopoulos and J. P. Aguilar, "An Optimization Framework for Driver Feedback Systems," *IEEE Transactions on Intelligent Transportation Systems*, vol. 14, no. 2, pp. 955–964, 2013.
- [2] K. Dresner and P. Stone, "Multiagent traffic management: a reservation-based intersection control mechanism," in *Proceedings of the Third International Joint Conference on Autonomous Agents and Multiagents Systems*, 2004, pp. 530–537.
- [3] —, "A multiagent approach to autonomous intersection management," *Journal of artificial intelligence research*, vol. 31, pp. 591–656, 2008.
- [4] A. de La Fortelle, "Analysis of reservation algorithms for cooperative planning at intersections," *13th International IEEE Conference on Intelligent Transportation Systems*, pp. 445–449, Sept. 2010.
- [5] S. Huang, A. Sadek, and Y. Zhao, "Assessing the Mobility and Environmental Benefits of Reservation-Based Intelligent Intersections Using an Integrated Simulator," *IEEE Transactions on Intelligent Transportation Systems*, vol. 13, no. 3, pp. 1201–1214, 2012.
- [6] I. H. Zohdy, R. K. Kamalanathsharma, and H. Rakha, "Intersection management for autonomous vehicles using iCACC," *2012 15th International IEEE Conference on Intelligent Transportation Systems*, pp. 1109–1114, 2012.
- [7] F. Yan, M. Dridi, and A. El Moudni, "Autonomous vehicle sequencing algorithm at isolated intersections," *2009 12th International IEEE Conference on Intelligent Transportation Systems*, pp. 1–6, 2009.
- [8] K.-D. Kim and P. Kumar, "An MPC-Based Approach to Provable System-Wide Safety and Liveness of Autonomous Ground Traffic," *IEEE Transactions on Automatic Control*, vol. 59, no. 12, pp. 3341–3356, 2014.
- [9] J. Rios-Torres and A. A. Malikopoulos, "A Survey on Coordination of Connected and Automated Vehicles at Intersections and Merging at Highway On-Ramps," *IEEE Transactions on Intelligent Transportation Systems*, vol. 18, no. 5, pp. 1066–1077, 2017.
- [10] H. Xia, K. Boriboonsomsin, and M. Barth, "Dynamic eco-driving for signalized arterial corridors and its indirect network-wide energy / emissions dynamic eco-driving for signalized arterial corridors and its indirect network-wide energy / emissions," *Journal of Intelligent Transportation Systems*, vol. 17, no. 1, pp. 37–41, 2013.
- [11] C. Roncoli, M. Papageorgiou, and I. Papamichail, "Traffic flow optimisation in presence of vehicle automation and communication systems – part ii: optimal control for multi-lane motorways," *Transportation Research Part C: Emerging Technologies*, vol. 57, pp. 260 – 275, 2015.
- [12] C. Roncoli, I. Papamichail, and M. Papageorgiou, "Hierarchical model predictive control for multi-lane motorways in presence of vehicle automation and communication systems," *Transportation Research Part C: Emerging Technologies*, vol. 62, pp. 117 – 132, 2016.
- [13] J. Rios-Torres, A. A. Malikopoulos, and P. Pisu, "Online Optimal Control of Connected Vehicles for Efficient Traffic Flow at Merging Roads," in *2015 IEEE 18th International Conference on Intelligent Transportation Systems*, 2015, pp. 2432–2437.
- [14] J. Rios-Torres and A. A. Malikopoulos, "Automated and Cooperative Vehicle Merging at Highway On-Ramps," *IEEE Transactions on Intelligent Transportation Systems*, vol. 18, no. 4, pp. 780–789, 2017.
- [15] I. A. Ntousakis, I. K. Nikolos, and M. Papageorgiou, "Optimal vehicle trajectory planning in the context of cooperative merging on highways," *Transportation Research Part C: Emerging Technologies*, vol. 71, pp. 464–488, 2016.
- [16] Y. Zhang, A. A. Malikopoulos, and C. G. Cassandras, "Optimal control and coordination of connected and automated vehicles at urban traffic intersections," in *Proceedings of the American Control Conference*, 2016, pp. 6227–6232.
- [17] L. Zhao, A. A. Malikopoulos, and J. Rios-Torres, "Optimal control of connected and automated vehicles at roundabouts: An investigation in a mixed-traffic environment," in *15th IFAC Symposium on Control in Transportation Systems*, 2018, pp. 73–78.
- [18] A. Stager, L. Bhan, A. A. Malikopoulos, and L. Zhao, "A scaled smart city for experimental validation of connected and automated vehicles," in *15th IFAC Symposium on Control in Transportation Systems*, 2018, pp. 120–135.
- [19] A. A. Malikopoulos, C. G. Cassandras, and Y. J. Zhang, "A decentralized energy-optimal control framework for connected automated vehicles at signal-free intersections," *Automatica*, vol. 93, pp. 244 – 256, 2018.
- [20] A. A. Malikopoulos, S. Hong, B. Park, J. Lee, and S. Ryu, "Optimal control for speed harmonization of automated vehicles," *IEEE Transactions on Intelligent Transportation Systems*, 2018 (in press).
- [21] R. Wiedemann, "Simulation des Strassenverkehrsflusses," Institut für Verkehrswesen der Universität Karlsruhe, UC Berkeley Transportation Library - Accession Number: 00896074, 1974.